Cell Host & Microbe
Article

The Release of Vaccinia Virus from Infected Cells Requires RhoA-mDia Modulation of Cortical Actin

Yoshiki Arakawa,[1] João V. Cordeiro,[1] Sibylle Schleich,[1] Timothy P. Newsome,[1] and Michael Way[1,*]
[1] Cell Motility Laboratory, Cancer Research UK, London Research Institute, 44 Lincoln's Inn Fields, London WC2A 3PX, UK
*Correspondence: michael.way@cancer.org.uk
DOI 10.1016/j.chom.2007.04.006

SUMMARY

Prior to being released from the infected cell, intracellular enveloped vaccinia virus particles are transported from their perinuclear assembly site to the plasma membrane along microtubules by the motor kinesin-1. After fusion with the plasma membrane, stimulation of actin tails beneath extracellular virus particles acts to enhance cell-to-cell virus spread. However, we lack molecular understanding of events that occur at the cell periphery just before and during the liberation of virus particles. Using live cell imaging, we show that virus particles move in the cell cortex, independently of actin tail formation. These cortical movements and the subsequent release of virus particles, which are both actin dependent, require F11L-mediated inhibition of RhoA-mDia signaling. We suggest that the exit of vaccinia virus from infected cells has strong parallels to exocytosis, as it is dependent on the assembly and organization of actin in the cell cortex.

INTRODUCTION

Vaccinia virus, a close relative of Variola virus, the causative agent of smallpox, is a large double-stranded DNA virus that undergoes a complex replication cycle in the cytoplasm of the infected cell (Harrison et al., 2004; Smith et al., 2003). Replication, which occurs in viral factories anchored at or near the microtubule-organizing center, results in the formation of two types of cytoplasmic virus particles, the intracellular mature virus (IMV) and the intracellular enveloped virus (IEV) (Harrison et al., 2004; Smith et al., 2003). IMV move throughout the cytoplasm in a bidirectional manner at speeds up to 3 $\mu m \cdot s^{-1}$, consistent with a microtubule-based transport mechanism (Ward, 2005). IEV are formed when IMV are wrapped by membrane cisternae derived from the trans-Golgi network or endosomal compartments containing a subset of integral viral membrane proteins (Harrison et al., 2004; Smith et al., 2003). IEV recruit the plus end-directed microtubule motor kinesin-1 (conventional kinesin) and are subsequently transported to the plasma membrane on microtubules in a saltatory fashion at speeds of up to 3 $\mu m \cdot s^{-1}$ (Geada et al., 2001; Hollinshead et al., 2001; Rietdorf et al., 2001; Ward and Moss, 2001a, 2001b). Fusion of the IEV with the plasma membrane results in the formation of the extracellular cell-associated enveloped virus (CEV) (Harrison et al., 2004; Smith et al., 2003). CEV that remain attached to the cell are able to induce an outside-in signaling cascade to locally activate Src and Abl family kinases (Frischknecht et al., 1999; Newsome et al., 2004, 2006; Reeves et al., 2005). This activation results in the tyrosine phosphorylation of A36R (Frischknecht et al., 1999; Newsome et al., 2004, 2006), an integral vaccinia membrane protein that becomes localized in the plasma membrane beneath CEV (Röttger et al., 1999; Smith et al., 2002; van Eijl et al., 2000). Phosphorylation of A36R facilitates the release of kinesin-1 (Newsome et al., 2004), and the subsequent recruitment of a signaling complex consisting of Grb2, Nck, WIP (WASP-interacting protein), and N-WASP (Frischknecht et al., 1999; Moreau et al., 2000; Scaplehorn et al., 2002; Snapper et al., 2001; Zettl and Way, 2002). The recruitment of N-WASP stimulates the actin-nucleating activity of the Arp2/3 complex, resulting in actin tail formation beneath the CEV (Frischknecht and Way, 2001). The stimulation of actin tails then acts to enhance cell-to-cell spread of the virus (Cudmore et al., 1995, 1996; Hollinshead et al., 2001; Ward and Moss, 2001a).

It has been calculated that an IEV particle would take 5.7 hr to move 10 μm in the cytoplasm of an infected cell, in the absence of an active transport mechanism (Sodeik, 2000). Clearly, cell-to-cell spread of vaccinia would be extremely inefficient if the virus was only dependent on diffusion. Fortuitously for the virus, it has evolved the ability to use both microtubule- and actin-based motility during its exit from the infected cell. Although actin-based motility provides an extra advantage to the virus, it is microtubule-based transport that plays the most important role during the spread of infection. In the absence of microtubule transport, IEV would only be released when the cell undergoes lysis or when a virus particle encounters the plasma membrane due to a diffusion-driven process. Microtubule-based transport thus ensures that IEV particles are efficiently delivered to the plasma membrane, where they are ultimately released from the infected cell.

We have shown that vaccinia not only uses the microtubule cytoskeleton for its transport but also stimulates increased microtubule dynamics during infection (Arakawa et al., 2007 [this issue of *Cell Host & Microbe*]). Vaccinia achieves these changes through the action of F11L, which binds to RhoA and blocks its ability to signal to mDia

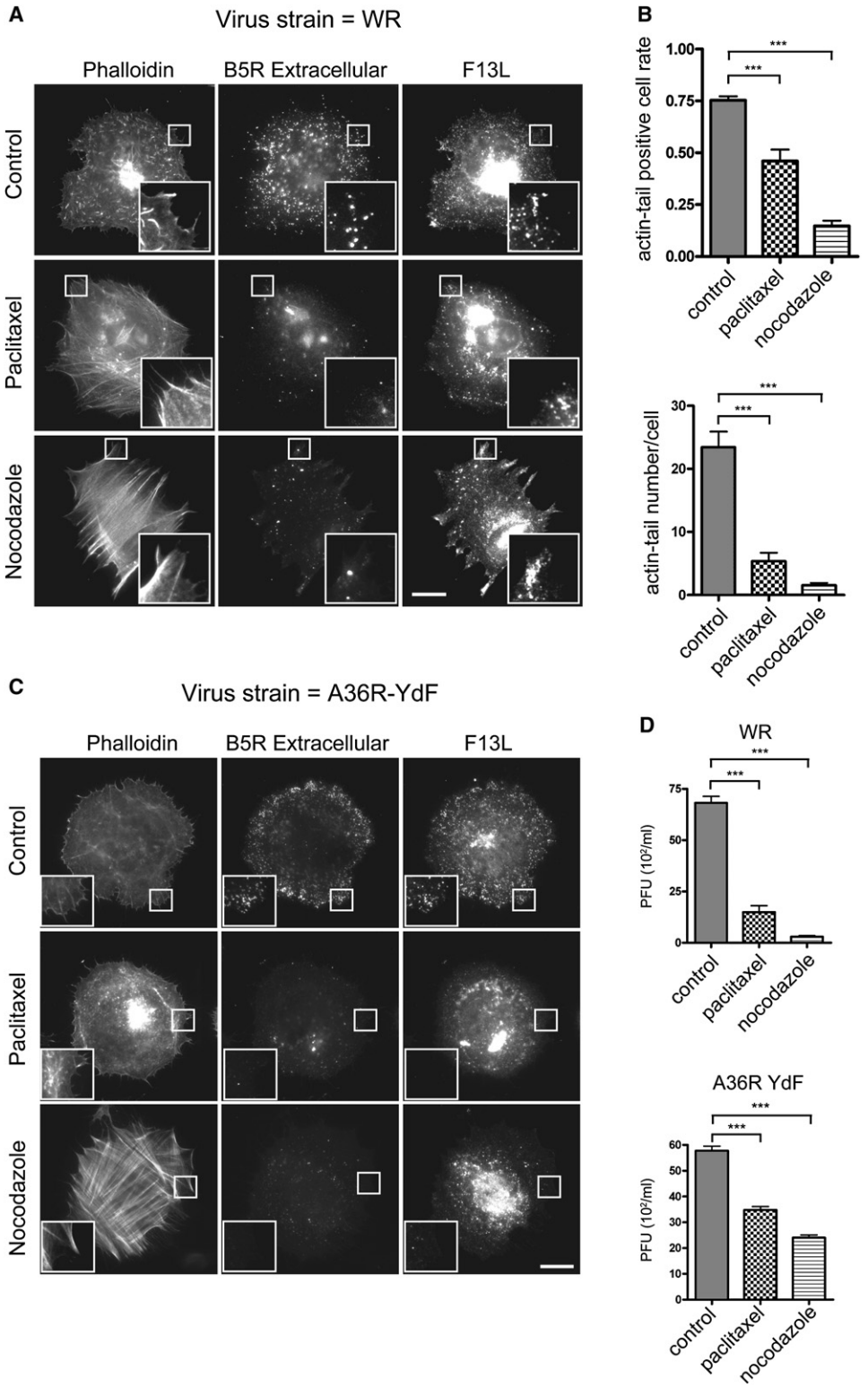

Figure 1. Stabilizing Microtubules Inhibits Virus Release

(A) Immunofluorescence images of the actin cytoskeleton, extracellular cell-associated enveloped virus (CEV = B5R), or intracellular and extracellular enveloped virus (IEV + CEV = F13L) particles in cells infected with WR for 10 hr after treatment with nocodazole or paclitaxel for the previous 2 hr. (B) Quantitative analyses of the actin tail positive cell rate and the number of actin tails in cells treated with nocodazole or paclitaxel.

(Arakawa et al., 2007; Valderrama et al., 2006). Infection also increases the targeting of microtubules to the cell periphery, suggestive of possible changes in the cell cortex. In this paper we sought to examine if changes in peripheral microtubule dynamics and their cortical targeting contribute to the exit of vaccinia from infected cells. Our observations have uncovered a role for RhoA-mDia signaling in the regulation of cortical actin and an actin-dependent movement of virus particles, which is likely to be a myosin-driven event, in the cell cortex prior to their release.

RESULTS

Microtubule Dynamics Promotes Release of Virus from Infected Cells

To test whether changes in microtubule dynamics might contribute to the spread of infection, we examined the effect of nocodazole and paclitaxel on vaccinia actin tail formation. We found that depolymerization of microtubules by 2 hr treatment with nocodazole, at 8 hr postinfection with Western Reserve (WR), results in a dramatic reduction in the number of actin tails and extracellular virus particles (CEV), indicative of a lack of IEV transport to the plasma membrane (Figures 1A–1C), as previously reported (Geada et al., 2001; Hollinshead et al., 2001; Ward and Moss, 2001a, 2001b). Consistent with these observations, reinfection plaque assays demonstrated that there was a corresponding decrease (>95%) in the number of infectious virus particles released into the media of nocodazole-treated cells (Figure 1D). Stabilization of microtubules with paclitaxel also resulted in a significant reduction in the number of WR-infected cells with actin tails and loss of extracellular CEV (Figures 1A–1C). There was also a corresponding ~60% reduction in the number of infectious virus particles released from paclitaxel-treated cells (Figure 1D). The effects of nocodazole and paclitaxel on virus release are not dependent on actin tail formation during WR infection. Treatment with either drug also reduced the number of extracellular CEV and infectious virus particles released into the media from cells infected with the recombinant virus strain A36R-YdF, which is unable to induce actin tails (Figures 1C and 1D).

The effects of nocodazole on CEV formation and virus release are readily explained by a lack of microtubule-dependent transport during both the formation of IEV and their subsequent transport to the cell periphery. A similar defect in microtubule-dependent transport of IEV to the plasma membrane could also account for the effects of paclitaxel treatment if kinesin-1 is unable to move on stabilized microtubules. However, this does not appear to be the case, as video analysis reveals that YFP-tagged IEV are still transported along microtubules in the presence of paclitaxel (Figure 2A; Movie S1 in the Supplemental Data available with this article online). It was noticeable, however, that the characteristic accumulation of virus particles at the edge of infected cells was absent in paclitaxel-treated cells (Figure 2A; Movie S1). Focusing on the bottom of paclitaxel-treated cells reveals that IEV particles are dispersed throughout the cell and also had great difficulty in approaching to within ~4 μm of the plasma membrane at the edge of the cell (Figure 2A).

The region immediately beneath the plasma membrane, which is known as the cell cortex, consists of a dense meshwork of actin filaments. One possible explanation for the effects of paclitaxel on intracellular virus distribution is that stabilization of microtubule cytoskeleton results in the reorganization of the actin in the cell cortex, which then acts as a barrier to prevent the virus from reaching the plasma membrane. To explore this hypothesis, we examined whether modulation of actin dynamics by the addition of Latrunculin B would rescue the effects of paclitaxel on virus release. We found that inhibition of actin polymerization with low concentrations of Latrunculin B (0.1 μM) could partially rescue the release of infectious virus particles from paclitaxel-treated cells (Figure 2B). Our observations are consistent with the hypothesis that the organization of cortical actin regulates the ability of the virus to reach the plasma membrane during its release.

Virus Release Involves an Actin-Dependent Event in the Cell Cortex

It is well established that the actin cytoskeleton plays an important role at multiple stages during exocytosis. We therefore wondered whether the release of virus particles at the plasma membrane is also dependent on actin, given they are a similar dimension to secretory granules. We found that a 2 hr treatment with a low (0.1 μM) concentration of Latrunculin B at 8 hr postinfection did not affect the number of WR-infected cells with actin tails or inhibit release of infectious virus particles into the media (Figure 2C). Indeed, video analysis and quantitative analysis of peripheral virus distribution reveals that this low concentration of Latrunculin B actually stimulates movement of virus particles in the cell periphery toward the plasma membrane (Figures 2D and 2E; Movie S2). In contrast, a similar treatment with high (1 μM) concentration of Latrunculin B was found to reduce the number of actin tails and the release of infectious virus particles (Figure 2C). Treatment of WR-infected cells with Cytochalasin D, which, in contrast to Latrunculin B, can cap the fast-growing end of actin filaments, in addition to sequestering actin monomers, was found to have more potent effects on the inhibition of actin tails and virus release (Figure 2C). Our observations indicate that virus release is dependent on the organization and dynamics of the actin cytoskeleton in the cell cortex.

(C) Representative immunofluorescence images of cells infected with the A36R-YdF strain of vaccinia, which is deficient in actin tail formation, reveal that treatment with nocodazole or paclitaxel results in loss of extracellular virus particles.
(D) Quantitative analyses of the number of infectious particles released from WR- and A36R-YdF-infected cells treated with the indicated drug. Error bars represent SEM; ***$p < 0.0001$. All scale bars, 20 μm.

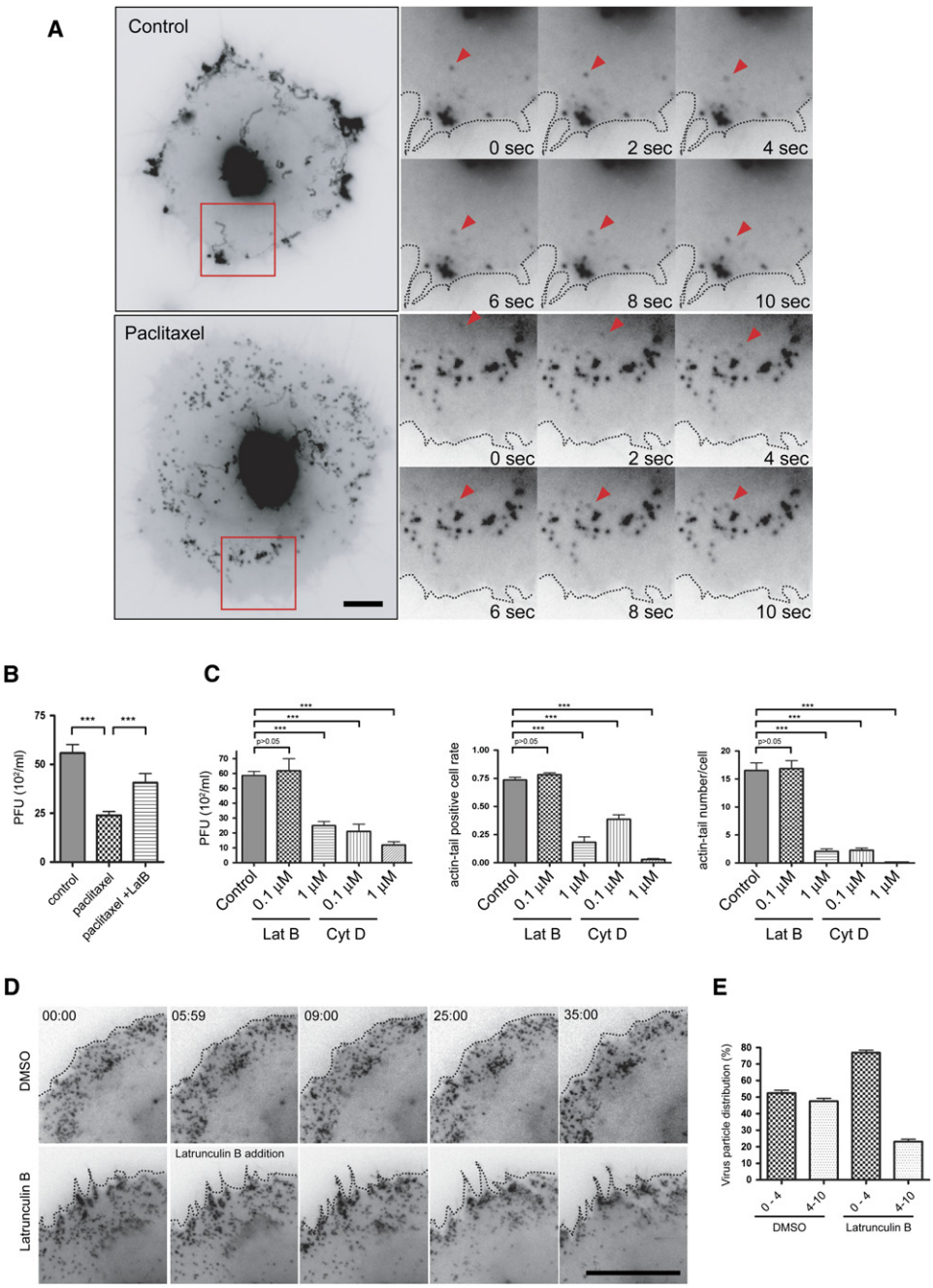

Figure 2. Actin Cytoskeleton Organization Modulates Virus Release

(A) Microtubule-dependent movement of intracellular enveloped virus (IEV) visualized with A36R-YdF-YFP with or without paclitaxel treatment. Whole-cell panel shows IEV virus particle distribution and tracks over 56 s, while the smaller panels represent movie stills from the highlighted area (see Movie S1).

(B) Quantitative analyses of the number of infectious particles released from WR-infected cells treated with the indicated drug.

(C) Quantitative analyses of the number of infectious particles released from WR-infected cells treated with the indicated drug (left). Quantitative analyses of the actin tail positive cell rate and the number of actin tails in cells treated with the indicated drug (middle, right).

(D) Time-lapse images of the periphery of a cell infected with the A36R-YdF-YFP virus reveal that addition of 0.1 μM Latrunculin B but not DMSO stimulates rapid movement of IEV virus particles to the plasma membrane (see Movie S2).

(E) Analyses of the number of virus particles 0–4 and 4–10 μm from the cell margin after a 5 min treatment with 0.1 μM Latrunculin B or DMSO in A36R-YdF-infected cells.

Error bars represent SEM; ***$p < 0.0001$. All scale bars, 20 μm.

Actin-Dependent Movement of Virus Particles in the Cell Cortex

To obtain more insights into the nature of virus particle movements occurring in the cell periphery, we performed video analysis at a higher sampling frequency on cells infected with the A36R-YdF virus, which cannot make actin tails. In the absence of drug treatments, we found that there were two distinct types of virus movement in addition to static virus particles (Figure 3A; Movies S3–S5). The first type of movement, which tended to occur over longer distances and in linear fashion, had an average speed of 1.06 ± 0.24 μm/s (n = 87), consistent with microtubule-based transport. The second form of motility, which was more random and tended to occur closer to the edge of the cell, had an average speed of 0.35 ± 0.1 μm/s (n = 301). When cells were treated with paclitaxel, there was a noticeable reduction in the second form of motility (Figure 3A; Movie S3). This paclitaxel-mediated inhibition of movement could be reversed by addition of low concentrations of Latrunculin B (Figure 3A; Movie S3). Consistent with these live observations, we found that low concentrations of Latrunculin B could partially rescue the effects of paclitaxel on the distribution of virus particles in the cell periphery (Figure 3B). The speed and behavior of this second form of virus motility is highly suggestive of an actin-based transport. To confirm this hypothesis, we examined the effect of modulating actin dynamics on virus particle movements in the cell periphery. We found that depolymerization or stabilization of actin filaments with Cytochalashin D or Jaspaklinolide, respectively, results in an increase in the number of static particles and reduction in the number of the slow random virus movements (Figure 3C; Movies S4 and S5).

The observation that addition of paclitaxel inhibits actin-dependent virus movements in the cell periphery suggests that microtubule dynamics is linked to regulation of cortical actin. This is not unexpected given the intimate and reciprocal relationship between microtubule and actin cytoskeletons. Live imaging and quantitative analysis on infected cells expressing YFP-actin reveal that addition of paclitaxel stimulates actin polymerization in cell cortex (Figures 3D and 3E). The ability of paclitaxel to stimulate actin polymerization in the cortex of infected cells is highly suggestive of RhoA activation. Quantitative western blot analysis of Rhotekin-pull-down assays on extracts from WR-infected cells treated with paclitaxel confirmed that stabilization of microtubules increases the level of GTP-bound Rho at 8 hr postinfection (Figure 3F). Our observations suggest that the organization of cortical actin regulates an actin-dependent transport step in the cell cortex, which is required for virus particles to reach the plasma membrane.

Loss of RhoA Signaling Facilitates Virus Release

Given the ability of paclitaxel to activate RhoA and stimulate peripheral actin polymerization, we investigated whether RhoA signaling also regulates virus release. We found that expression of constitutively active RhoA-V14, but not dominant-negative RhoA-N19, at 8 hr postinfection dramatically reduces the number of CEV and their associated actin tails in WR-infected cells (Figures 4A and 4B). Reinfection assays confirmed that expression of RhoA-V14 also reduces the release of infectious virus particles (Figure 4C). Consistent with our earlier observations, we found that the effect of RhoA-V14 expression on virus release could be reversed by treating infected cells with low concentrations of Latrunculin B (Figure 4C). Likewise, expressing dominant-negative RhoA-N19 neutralized the effects of paclitaxel treatment on virus release (Figure 4C). Our observations suggest that RhoA signaling plays an important role in regulating the organization of the actin cytoskeleton during virus release.

F11L-Mediated Inhibition of RhoA Enhances Virus Release

Our observations suggest that RhoA signaling acts to inhibit virus release by stimulating actin polymerization in the cell cortex. However, during the course of a normal infection, the viral protein F11L binds to RhoA to inhibit its downstream signaling (Arakawa et al., 2007; Valderrama et al., 2006). Our previous observations have demonstrated that F11L is required for efficient virus particle assembly. Consequently, to examine if F11L-mediated inhibition of RhoA signaling is required for virus release, we examined the consequences of overexpressing an F11L mutant (F11L-VK) that is unable to bind RhoA. We found that overexpression of F11L-VK, at 8 hr postinfection, results in a dramatic reduction in the number of extracellular virus particles (CEV) and actin tails in WR-infected cells (Figures 5A–5C). There was also a corresponding reduction in the number of infectious virus particles released into the media (Figure 5D). The effects of F11L-VK on virus release could be rescued by inhibiting RhoA signaling with TAT-C3. F11L-VK mutant appears to be acting as a dominant negative to prevent the F11L-mediated inhibition of RhoA signaling during vaccinia infection. Our previous observations have shown that F11L binds RhoA in a similar fashion to ROCK (Valderrama et al., 2006), suggesting that F11L may also function as a dimer. We therefore performed pull-down assays to examine if F11L can interact with itself. We found that GST-tagged F11L and F11L-VK were equally effective pulling down endogenous F11L from WR-infected cells (Figure 5E). We believe that the formation of F11L and F11L-VK complexes that are unable to inhibit RhoA signaling is likely to account for the dominant-negative effect of F11L-VK overexpression on virus release.

RhoA Signaling to mDia Regulates Cortical Actin and Virus Release

Previous studies have established a role for Myosin II during exocytosis. As Myosin II is downstream of RhoA-ROCK signaling, we wondered whether ROCK participates in regulating cortical actin during virus release. We found that the formation of actin tails and release of infectious virus particles from paclitaxel-treated cells is rescued by inhibiting RhoA signaling with TAT-C3 exoenzyme (Figures 6A–6C). In contrast, inhibition of ROCK with Y-27632 did

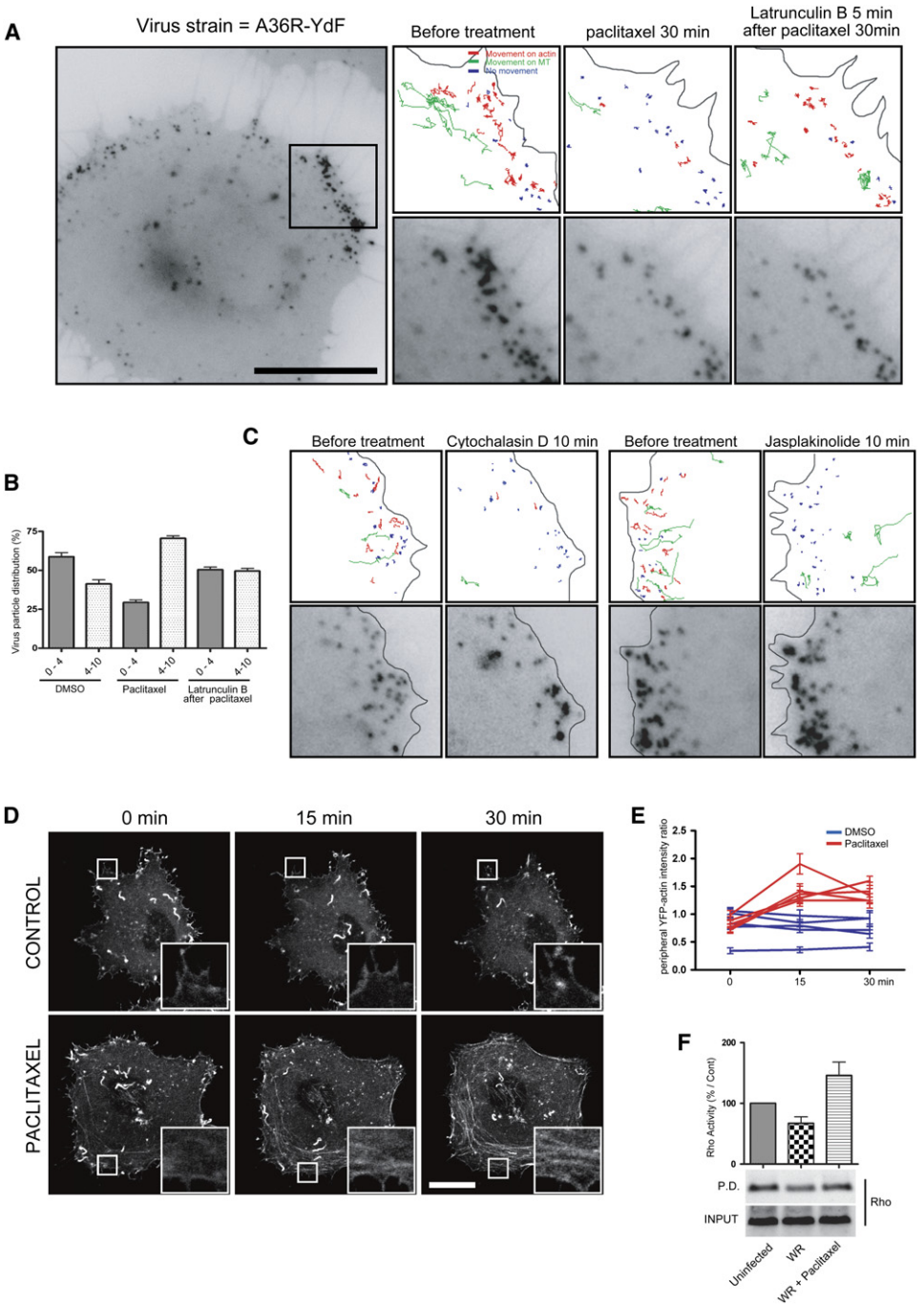

Figure 3. Actin-Dependent Movement of Virus Particles in the Cell Periphery

(A) Movement of intracellular enveloped virus (IEV) visualized with A36R-YdF-YFP in the cell cortex before and after first paclitaxel addition and second 0.1 μM Latrunculin B. Smaller panels represent movie stills from the highlighted area in main cell. Color-coded tracks of the movements of virus particles over 26 s for each drug regime are indicated above each movie still (see Movie S3).

(B) Quantitative analyses of the number of virus particles 0–4 and 4–10 μm from the cell margin after treatment with DMSO for 30 min, paclitaxel for 30 min, or 0.1 μM Latrunculin B (5 min) following 30 min incubation in paclitaxel in A36R-YdF-infected cells.

(C) Color-coded tracks of IEV particle movements in the cell cortex over 26 s before and after the indicated drug (see Movies S4 and S5).

(D) Confocal laser scanning images of actin cytoskeleton at the bottom of WR-infected cells expressing YFP-actin confirm that treatment with paclitaxel stimulates actin polymerization in the cell periphery.

(E) Quantitative analysis of the relative intensity of cortical actin in WR-infected cells expressing YFP-actin treated with DMSO or paclitaxel.

(F) Immunoblot and quantitative analysis of Rho activity in WR-infected cells treated with paclitaxel.

Error bars represent SEM. All scale bars, 20 μm.

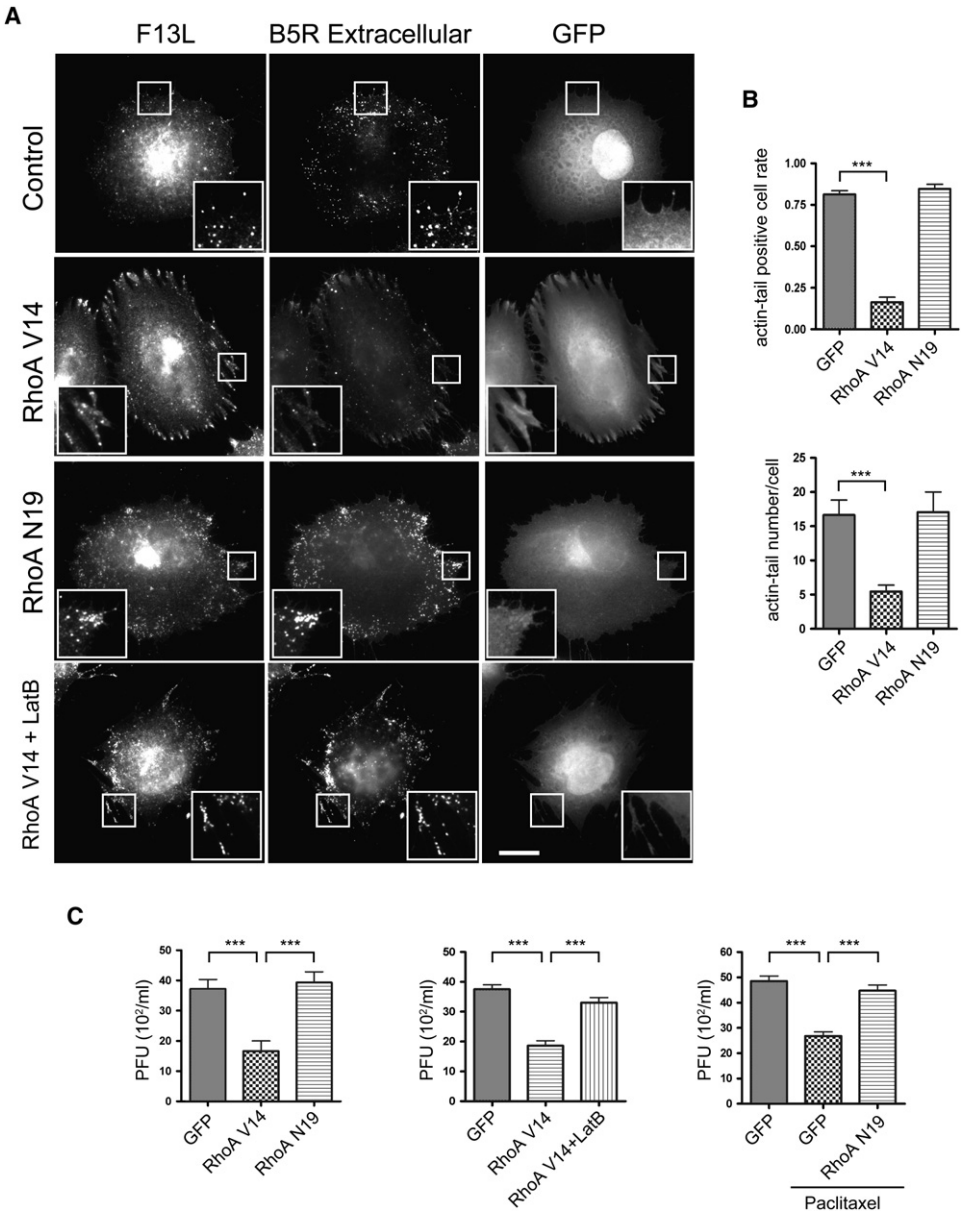

Figure 4. RhoA Signaling Inhibits Virus Release by Stimulating Actin Polymerization

(A) Immunofluorescence images of extracellular cell-associated enveloped virus (CEV = B5R) or intracellular and extracellular enveloped virus (IEV + CEV = F13L) particles in WR-infected cells expressing GFP-tagged RhoA V14 and RhoA N19 and treated with 0.1 μM Latrunculin B.

(B) Quantitative analyses of the actin tail positive cell rate and the number of actin tails in WR-infected cells expressing the indicated GFP-tagged protein.

(C) Quantitative analyses of the number of infectious virus particles released from WR-infected cells expressing the indicated protein and treated with the indicated drugs.

Error bars represent SEM; ***$p < 0.0001$.

not rescue the effects of paclitaxel on WR-infected cells (Figures 6A–6C). Given the absence of an effect of Y-27632 on paclitaxel-treated cells, we examined whether expression of active mDia1 (mDia1 ΔN3) might inhibit release of infectious virus particles. We found that expression of the active form of mDia1 but not ROCK1 (ROCK1 Δ3) reduced the number of extracellular virus particles and actin tails in WR-infected cells (Figures 7A and 7B). Active mDia1 also reduced the number of infectious particles released into the media (Figure 7C). The effect of active mDia1 on virus release could be rescued by treating infected cells with low concentrations of Latrunculin B (Figure 7C). To obtain further insights into the role of RhoA-mDia signaling during virus release, we performed video analysis on infected cells expressing active RhoA or mDia1 at 8 hr postinfection (Figure 7D; Movie S6). In

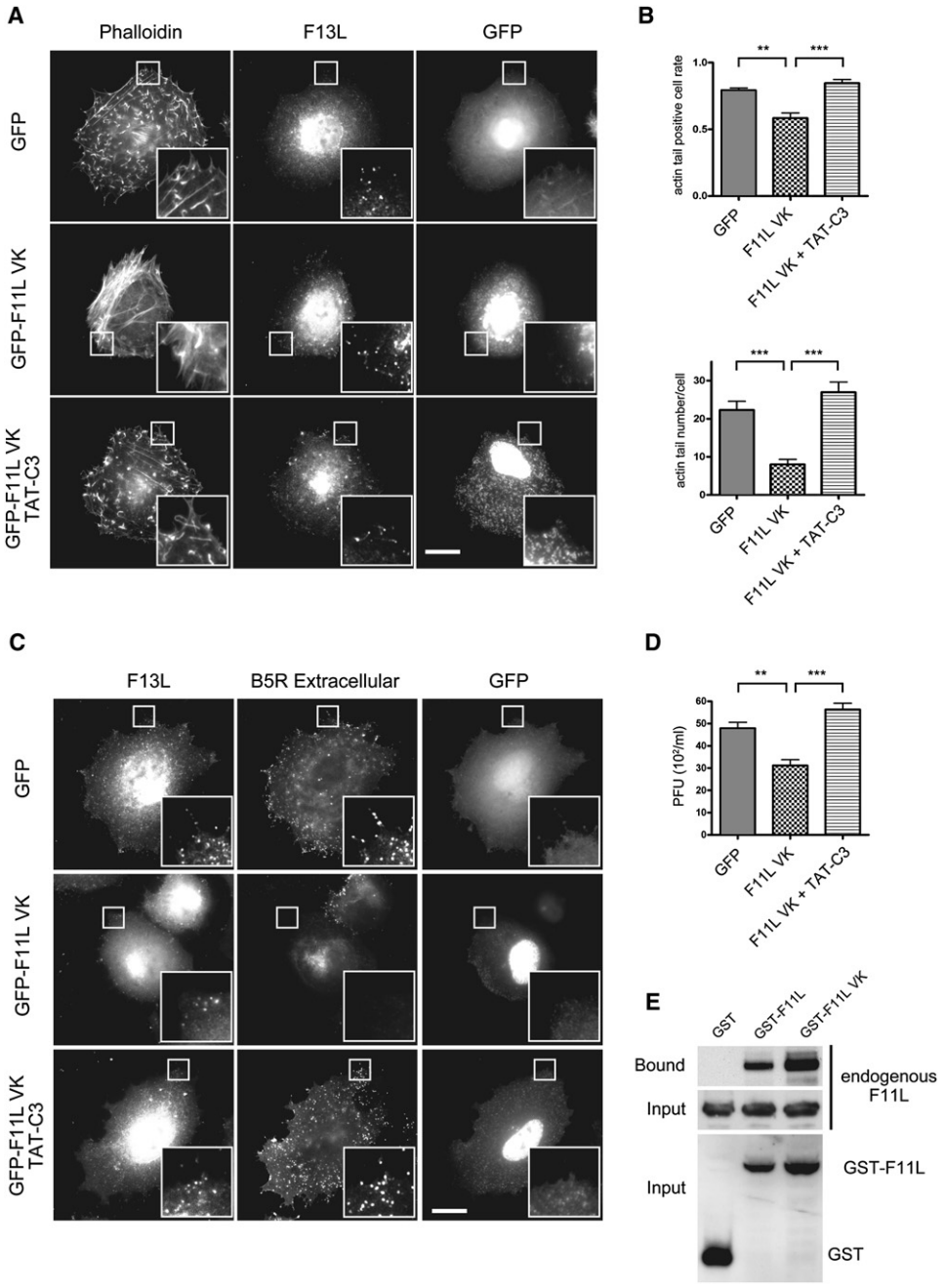

Figure 5. An Interaction of F11L with RhoA Is Required to Promote Virus Release

(A) Representative immunofluorescence images of the actin cytoskeleton, CEV (B5R), or IEV and CEV (F13L) particles in WR-infected cells expressing GFP-F11L-VK, which cannot bind RhoA, with or without TAT-C3 treatment.

(B) Quantitative analyses of the actin tail positive cell rate and the number of actin tails in WR-infected cells expressing GFP-F11L-VK with or without TAT-C3 treatment.

(C) Immunofluorescence images of CEV (B5R) and IEV + CEV (F13L) in WR-infected cells expressing GFP-F11L-VK in the presence or absence of TAT-C3.

(D) Quantitative analyses of the number of infectious particles released from WR-infected cells expressing GFP-F11L-VK in the presence or absence of TAT-C3.

(E) Immunoblot analyses of pull-down assays reveal that GST-tagged F11L or F11L-VK is able to interact with endogenous F11L during WR infection. Error bars represent SEM; $^{**}p < 0.001$, $^{***}p < 0.0001$.

contrast to controls, we found that virus particles did not accumulate at the edge of cells expressing active RhoA or mDia1. It was also apparent that virus particles in the cell periphery were also largely static and did not undergo slow actin-dependent movements (Figure 7D). Taken together, our observations suggest that F11L-mediated

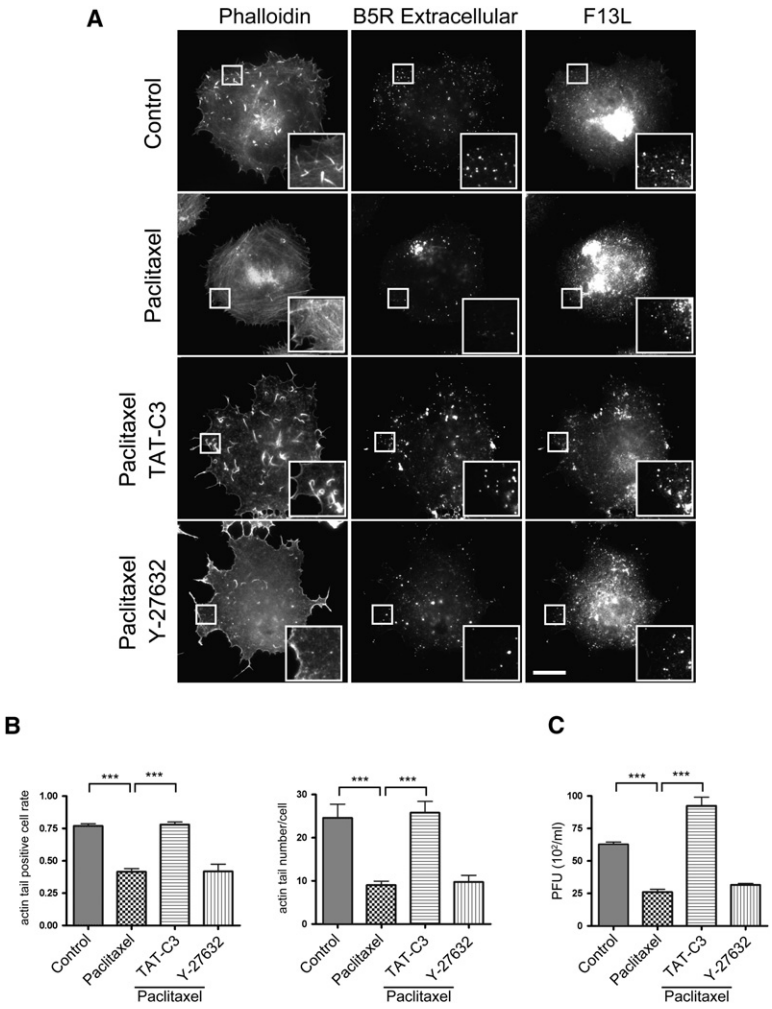

Figure 6. ROCK Is Not Required for Microtubule-Dependent Virus Release

(A) Immunofluorescence images of the actin cytoskeleton, CEV (B5R), or IEV and CEV (F13L) particles in WR-infected cells treated with the indicated drugs or TAT-C3.

(B) Quantitative analyses of the actin tail positive cell rate and the number of actin tails in WR-infected cells in the various treatments.

(C) Quantitative analysis of the number of infectious particles released from WR-infected cells treated with the indicated drugs.

Error bars represent SEM; ***$p < 0.0001$.

inhibition of RhoA-mDia signaling leads to changes in organization of actin in the cell cortex, which acts to facilitate virus release (Figure 7E).

DISCUSSION

The Actin Cortex Regulates Virus Release

The ability of virus particles to reach the cell periphery and fuse with the plasma membrane is critical for the cell-to-cell spread of vaccinia virus. It is therefore not surprising that treatment with nocodazole reduced accumulation of particles in cell periphery, actin tail formation, and release of infectious virus particles given the importance of microtubules in IEV transport to the plasma membrane (Geada et al., 2001; Hollinshead et al., 2001; Rietdorf et al., 2001; Ward and Moss, 2001a, 2001b). We did not, however, expect to obtain similar results when microtubules were stabilized by paclitaxel. The effects of paclitaxel are not related to microtubule-dependent transport, as IEV moved toward the cell periphery at speeds indistinguishable from untreated cells (data not shown). This is consistent with recent observations demonstrating that stabilization of microtubules via acetylation promotes rather than inhibits kinesin-1 binding and cargo transport (Reed et al., 2006). Instead, our observations indicate that the effects of paclitaxel on virus release are related to its ability to stimulate RhoA-dependent actin polymerization in the cell cortex.

The cell cortex immediately beneath the plasma membrane consists of an extremely dense arrangement of actin filaments. These actin filaments are constantly being remodeled in response to numerous signaling pathways to accommodate the cells ever-changing needs. The organization and dynamics of actin in the cell cortex plays an important role in the normal functioning of the cell, as it helps to maintain the cell shape and provides the driving force for cell motility. Remodeling of cortical actin is also essential for endocytosis and exocytosis (Eitzen, 2003; Engqvist-Goldstein and Drubin, 2003; Malacombe et al., 2006; Qualmann and Kessels, 2002). Notwithstanding its importance in membrane trafficking, cortical actin actually represents a significant barrier to exocytosis, as it prevents vesicles and secretory granules from reaching and fusing with the plasma membrane.

Vaccinia virus particles are of similar dimension to secretory granules (Cyrklaff et al., 2005). It is therefore not

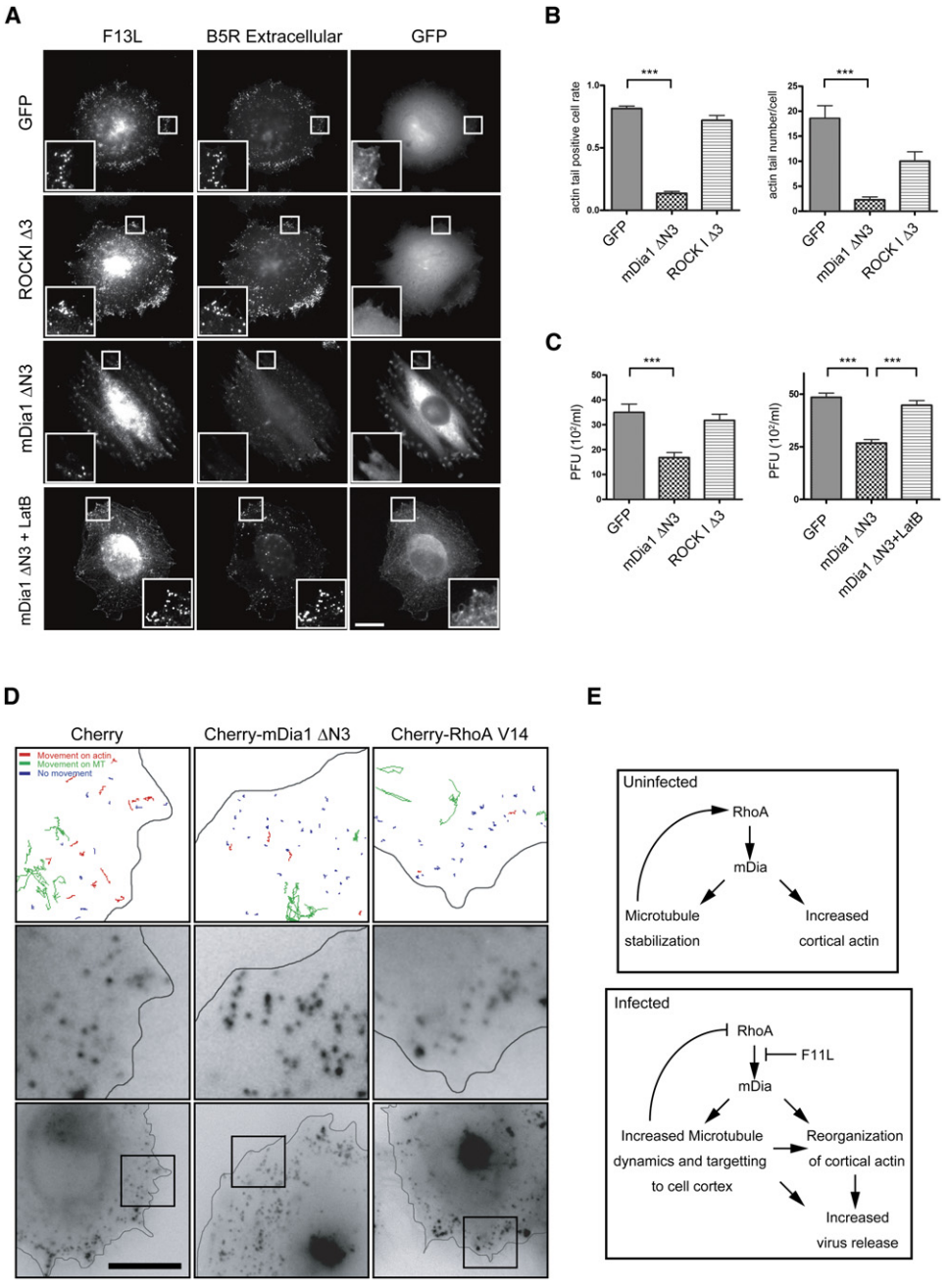

Figure 7. mDia-Mediated Actin Polymerization Inhibits Virus Particle Release

(A) Immunofluorescence images of the actin cytoskeleton, CEV (B5R), or IEV and CEV (F13L) particles in WR-infected cells expressing GFP-tagged active forms of mDia1 (mDia1 ΔN3) and ROCK1 (ROCK1 Δ3), in the presence or absence of 0.1 μM Latrunculin B.

(B) Quantitative analyses of the actin tail positive cell rate and the number of actin tails in WR-infected cells expressing mDia1 ΔN3 and ROCK1 Δ3.

(C) Quantitative analyses of the number of infectious particles released from WR-infected cells expressing the indicated GFP-tagged protein in the presence or absence of 0.1 μM Latrunculin B.

(D) Movement of IEV particles in cells infected with A36R-YdF-YFP and expressing mDia1 ΔN3 and RhoA V14. Smaller panels represent movie stills from the highlighted area in main cell. Color-coded tracks of the movements of virus particles over 26 s for each drug regime are indicated above each movie still (Movie S6).

(E) Schematic representation of F11L-mediated inhibition of RhoA-mDia signaling, which results in increased microtubules dynamics and changes in cortical actin that promote virus particle release.

Error bars represent SEM; ***$p < 0.0001$.

surprising that the actin cortex would act to prevent the virus reaching the plasma membrane prior to release. We found that low concentrations of Latrunculin B rescued the inhibitory effects of paclitaxel treatment on virus release, presumably as the drug reduces the physical barrier, by inducing changes in the organization of cortical actin. Low concentrations of Latrunculin B have also been found to stimulate exocytosis in a variety of cell types (Eitzen, 2003; Malacombe et al., 2006). Low concentrations of Latrunculin B clearly do not inhibit actin polymerization, as in WR-infected cells the virus is still able to stimulate formation of actin tails at a similar level to untreated cells. In contrast, high concentrations (1 μM) of Latrunculin B or low concentrations (0.1 μM) of Cytochalasin D suppress both actin tail formation and virus release. The difference in potency between Latrunculin B and Cytochalasin D, at low concentrations, reflects their different modes of action. Both bind actin monomers to reduce the pool of polymerization-competent actin (Coue et al., 1987). However, only Cytochalasin D can bind directly to the faster growing or barbed end of actin filaments to inhibit their elongation (Sampath and Pollard, 1991). The simplest explanation for our observations is that a dynamic actin cytoskeleton is required for virus release. The question is at what stage during virus release dynamic actin cytoskeleton is involved.

What Drives Peripheral Virus Movement?

During secretory granule exocytosis, the actin cortex is thought to undergo local remodeling to allow myosin motors to transport their associated cargoes to the plasma membrane (Soldati and Schliwa, 2006). On reaching the edge of the cell, the actin cytoskeleton is then thought to help anchor the secretory granules to the plasma membrane. Finally, actin polymerization drives their fusion and release (Eitzen, 2003; Malacombe et al., 2006). Given their size and need for directed transport, it is likely that related steps are also occurring during release of IEV particles. Indeed, it has been calculated that it would take over 30 min for an IEV to move 1 μm in the cytoplasm, let alone in the dense actin cortex (Sodeik, 2000). Our observations have revealed that IEV particles exhibit two distinct types of movement in the cell periphery. The first occurs over longer distances and is linear in nature, consistent with microtubule-based transport. The average speed (1.06 ± 0.24 μm/s) of this movement agrees well with our previous observations of IEV moving on microtubules in the cell body (0.8 ± 0.2 μm/s) (Rietdorf et al., 2001). The second form of movement, which is considerably slower (0.35 ± 0.1 μm/s) and agrees well with myosin-driven motility, tends to be more random in nature and occurs closer to the edge of the cell. Similar types and speeds of movements have also been described for secretory granules in the cell cortex (Lang et al., 2000; Manneville et al., 2003; Rudolf et al., 2001).

As observed for secretory granules, we found that the slow random IEV particle movements in the cell periphery are inhibited by drug-mediated depolymerization or stabilization of the actin cytoskeleton. The need for a dynamic actin cytoskeleton may point to these movements being driven by actin polymerization. Indeed, previous observations have demonstrated that intracellular vesicular trafficking can be driven by Arp2/3-dependent actin polymerization in a manner that is analogous to that used by a number of intracellular pathogens such as *Listeria* (Benesch et al., 2002; Kaksonen et al., 2000; Rozelle et al., 2000; Taunton et al., 2000). However, we do not think that is the case for vaccinia, as peripheral IEV particle movements (0.35 ± 0.1 μm/s) are about twice as fast as the rate at which CEV particles move on actin tails (0.18 ± 0.05 μm/s) (Rietdorf et al., 2001). In addition, we have never observed an enrichment of actin on IEV particles during infections with the A36R-YdF virus, which is unable to stimulate actin tails.

A number of reports have also demonstrated that the actin-dependent movement of endosomes involves RhoB signaling through mDia (Fernandez-Borja et al., 2005; Gampel et al., 1999; Sandilands et al., 2004; Wallar et al., 2007). In addition, RhoD has been shown to regulate the dynamics of Rab5-positive endosomes through mDia and Src (Gasman et al., 2003). In contrast to these studies, we have never observed RhoA or mDia on virus particles moving in the cell periphery or on microtubules. In addition, we also found that inhibition of RhoA by TAT-C3 actually stimulates virus release (data not shown). While we cannot formally rule out a role for RhoA-mDia signaling during virus trafficking, we believe that our data are more consistent with a model in which peripheral IEV particle movements are driven by a myosin motor, combined with rearrangements of the cortical actin, which are regulated by RhoA-mDia signaling.

RhoA-mDia Signaling Regulates Cortical Actin

Although the actin cortex plays an important role in the life of a cell, we know surprisingly little at the molecular level about how its organization and dynamics are controlled. Previous observations have demonstrated that Cdc42 and Rac play an important role in exocytosis in a variety of situations and cell types (Eitzen, 2003; Malacombe et al., 2006; Ridley, 2001; Symons and Rusk, 2003). More recently, TC10, a Cdc42 homolog, has also been shown to regulate exocytosis of Glut4 during insulin-stimulated signaling (Kawase et al., 2006; Symons and Rusk, 2003). Our observations in vaccinia-infected cells suggest that RhoA signaling through mDia plays an important role in regulating the organization of cortical actin during exocytosis. Our findings are consistent with results demonstrating that RhoA signaling is required for assembly of cortical actin after cell blebbing (Charras et al., 2006). Recent observations have also shown that Dia-interacting protein (DIP) modulates cortical actin during cell blebbing by interfering with mDia2-mediated actin organization (Eisenmann et al., 2007). During infection we envisage that F11L-mediated inhibition of RhoA signaling to mDia results in changes in the overall organization of cortical actin that allow the virus to reach the plasma membrane, probably by a myosin-driven event. These changes may also explain why microtubules have an increased tendency to reach the cell periphery during WR infection

(Arakawa et al., 2007), as the cortical actin no longer represents a physical barrier to reaching the plasma membrane. Our observations also provide an explanation of why vaccinia has evolved mechanisms to suppress RhoA signaling during infection.

Our future studies will be aimed at elucidating which one of the many myosin motors involved in vesicular traffic might drive IEV movements in the cell cortex. A detailed understanding of the temporal and ultrastructural changes occurring in the actin cortex during infection will also be required to fully understand exactly how vaccinia escapes from the cell and whether actin polymerization also facilitates fusion of the virus with the plasma membrane.

EXPERIMENTAL PROCEDURES

Infection, Transfection, and Drug Treatments

HeLa cells on fibronectin-coated coverslips or dishes were infected with WR or the recombinant vaccinia virus strains A36R-YdF (Rietdorf et al., 2001), A36R-YdF-YFP, and YFP-A3L and processed for immunofluorescence or immunoblot analysis 8–10 hr postinfection as described previously (Arakawa et al., 2007). Infected cells were also transfected with pEL expression vectors or treated with drugs (paclitaxel [10 μM], nocodazole [10 μg/ml], TAT-C3 exoenzyme [10 μg/ml], Y-27632 [25 μM], Jasplakinolide [1 μM], Cytochalasin D [0.1–1 μM], or Latrunculin B [0.1–1 μM]) at 8 hr postinfection as required and processed for immunofluorescence or immunoblot analysis 2–3 hr later (Arakawa et al., 2007).

Construction of Recombinant A36R-YdF-YFP and YFP-A3L Vaccinia Virus

The DNA corresponding to the open reading frame of A36R but lacking the stop codon and 327 bp upstream of the gene (left arm [LA]) was amplified by PCR using DNA of the viral strain A36R-YdF DNA (ref). The resulting product was cloned into the HindIII-NotI sites of pBS SKII containing YFP (in the NotI-BamHI) to generate LA-A36R-YdF-YFP. In an independent reaction, the DNA corresponding to 325 bp downstream of the A36R ORF (right arm [RA]) was cloned into the BamHI-NotI sites of pBS SKII to generate pBS SKII-RA. The LA-A36R-YdF-YFP insert was subsequently moved into the pBS SKII-RA using the HindIII-BamHI restriction sites, which flank the insert to generate the final targeting vector LA-A36R-YdF-YFP-RA in pBS SKII. A fragment of genomic WR DNA, the 200 bp upstream of A3L, was amplified by PCR and cloned into the KpnI site of pEL-YFP-A3L to create the targeting LA-YFP-A3L in pBS SKII. The A36R-YdF-YFP and YFP-A3L targeting vectors were transfected into ΔA36R and WR virus-infected cells, respectively. Recombinant viruses encoding their respective YFP-tagged proteins were isolated by successive rounds of plaque purification. The fidelity of the final recombinant virus strains was confirmed by sequencing, immunofluorescence, plaque size comparison, and reinfection assays (Figures S1 and S2).

Generation of YFP-β-Actin Cell Lines

Lentiviruses of YFP-tagged human β-Actin were created using Lentivirus systems (Rubinson et al., 2003). A fragment of pEYFP-β-Actin (Clontech, CA) was cloned into the NheI-BamHI site of pLL3.7-GFP to create pLL3.7-EYFP-β-Actin. HeLa cells stably expressing pEYFP-β-Actin were generated using these lentiviruses and were subsequently isolated by fluorescence-activated cell sorting.

Antibodies, Reagents, and Vector Construction

Antibodies against the viral protein B5R (19C2) (Hiller and Weber, 1985), F13L (Rietdorf et al., 2001), A36R (Röttger et al., 1999), and F11L (Valderrama et al., 2006) have been previously described. Antibodies were purchased as follows: Rho (-A, -B, -C) (55) (Upstate, NY); anti-GST antibody (Sigma-Aldrich, UK); goat Alexa Fluor 488, 568 conjugates to rabbit, rat, and mouse IgG (Molecular Probes, OR); goat Cy5 conjugates to rabbit and rat IgG (Jackson ImmunoResearch Laboratories, PA); goat HRP conjugates to rabbit and mouse IgG (Bio-Rad Laboratories, CA); goat IRDye 800CW conjugates to mouse IgG (LI-COR Corporate, NE). Alexa Fluor 568-phalloidin (Molecular Probes, OR), TAT-C3 exoenxyme (Sahai and Olson, 2006), Y-27632 (Calbiochem-Merck Biosciences, Germany), nocodazole, Latrunculin B, Cytochalasin D, paclitaxel, human plasma fibronectin (Sigma-Aldrich, UK), Rho Assay Reagents (Upstate, NY), and Jasplakinolide (Molecular Probes, OR, USA). All pEL vectors used in the manuscript to express proteins during vaccinia infection have been described previously (Arakawa et al., 2007; Valderrama et al., 2006). mCherry was provided by R.Y. Tsien (University of California, San Diego) (Shaner, et al., 2004). mDia1 ΔN3 and ROCK1 Δ3 were provided by S. Narumiya (Kyoto University, Kyoto, Japan) (Watanabe et al., 1999; Ishizaki et al., 1997). The vaccinia expression vector pEL-N-GST-3C was constructed by replacing the GFP with GST-3C in the pEL vector (Frischknecht et al., 1999). F11L, F11L-V305/K307 (F11L-VK) were subcloned into the pEL-N-GST-3C vectors.

Analysis of Peripheral Virus Particle Distribution

The number of virus (IEV and CEV) particles within five 4 μm wide rectangles up to 4.0 μm or 10.0 μm from the edge of the cell was counted in fixed cells labeled with the B5R antibody. Peripheral virus particle distribution was calculated as 0–4 μm and 4–10 μm in ten cells for each treatment.

Laser Scanning Microscopy and Fluorescence Microscopy

Confocal images from live cells stably expressing YFP-tagged human β-Actin were collected using a LSM 510 META system with Plan-Apochromat 63/1.40 Oil Ph3 lens (Carl Zeiss MicroImaging, Inc.). To quantify the relative intensity of cortical actin, a confocal slice corresponding to the bottom of the cell was collected at 0, 15, and 30 min after drug treatment. After background subtraction, five regions of interest (ROI, 4 × 4 μm square) were randomly placed in the cell periphery. The relative intensity of cortical actin was calculated as ROI/whole-cell intensity and showed mean ± SEM in five independent assays. To analyze IEV movement in the cell periphery, images from live cells infected with A36R-YdF-YFP strain, which is deficient in actin tail formation, were collected using a Cascade II 512B cooled CCD camera (Photometrics, AZ) on an Axiovert 200 equipped with a optovar 1.6, Plan-Apochromat 63/1.40 Oil Ph3 lens (Carl Zeiss, Germany). HeLa cells were imaged with stream acquisition (50 images in 26 s) at 8 hr postinfection. Alternatively, cells were imaged at 10 hr postinfection after transfection with pEL-Cherry expression constructs or addition of drugs 8 hr after the initial infection. Quantification and analysis of the behavior of IEV movement in cell periphery was performed using MetaMorph software (Molecular Devices Corporation, CA). Images were prepared for publication using Photoshop and Illustrator packages (Adobe, CA).

Fluorescence-Based Reinfection Assay

To measure the effects of drug addition or protein expression on virus release at 8 hr postinfection, we developed a fluorescence-based reinfection assay. HeLa cells in 24-well dishes were infected for 8 hr with YFP-A3L recombinant virus at an MOI of 5. Infected cells were washed twice and changed to new media (200 μl) with or without drugs as necessary. Alternatively, cells were transfected with pEL expression vectors 8 hr after infection, and new media were added 2 hr later. In both cases, 12 hr after the addition of new media cells were centrifuged and supernatant was removed. To assess virus release, the supernatant was diluted 200-fold and used to infect cells for 1 hr prior to agarose overlay for standard plaque assays. The number of fluorescent plaques was counted 24 hr later to measure the number of infectious virus particles released into the supernatant from the primary infection in the various conditions. For each individual experimental condition, triplicate assays were counted, in at least three independent

experiments. The fidelity of our reinfection assay with YFP-A3L strain was confirmed by the conventional reinfection assay using WR.

Statistical Analysis

Data are presented as mean ± standard error of the mean and were analyzed by ANOVA or Student's t test using Prism 4.0 (GraphPad Software, CA). A p value of <0.05 was considered statistically significant.

Supplemental Data

The Supplemental Data include two supplemental figures and six supplemental movies and can be found with this article online at http://www.cellhostandmicrobe.com/cgi/content/full/1/3/227/DC1/.

ACKNOWLEDGMENTS

We would like to thank Shuh Narumiya (Kyoto University, Kyoto, Japan), Erik Sahai (Cancer Research UK, London), and Roger Y. Tsien (University of California, San Diego) for reagents. We would like to thank the members of the Way lab, Richard Treisman, Erik Sahai, Sharon Tooze, and Stephane Gasman for constructive comments on the manuscript. This work was supported by Cancer Research UK (Y.A., J.V.C., S.S., T.P.N., and M.W.), and partially by the Human Frontier Science Program (T.P.N.).

Received: December 7, 2006
Revised: February 24, 2007
Accepted: April 18, 2007
Published: May 16, 2007

REFERENCES

Arakawa, Y., Cordeiro, J.V., and Way, M. (2007). F11L-mediated inhibition of RhoA-mDia signaling stimulates microtubule dynamics during vaccinia virus infection. Cell Host & Microbe *1*, this issue, 213–226.

Benesch, S., Lommel, S., Steffen, A., Stradal, T.E., Scaplehorn, N., Way, M., Wehland, J., and Rottner, K. (2002). Phosphatidylinositol 4,5-biphosphate (PIP2)-induced vesicle movement depends on N-WASP and involves Nck, WIP, and Grb2. J. Biol. Chem. *277*, 37771–37776.

Charras, G.T., Hu, C.K., Coughlin, M., and Mitchison, T.J. (2006). Reassembly of contractile actin cortex in cell blebs. J. Cell Biol. *175*, 477–490.

Coue, M., Brenner, S.L., Spector, I., and Korn, E.D. (1987). Inhibition of actin polymerization by latrunculin A. FEBS Lett. *213*, 316–318.

Cudmore, S., Cossart, P., Griffiths, G., and Way, M. (1995). Actin-based motility of vaccinia virus. Nature *378*, 636–638.

Cudmore, S., Reckmann, I., Griffiths, G., and Way, M. (1996). Vaccinia virus: A model system for actin-membrane interactions. J. Cell Sci. *109*, 1739–1747.

Cyrklaff, M., Risco, C., Fernandez, J.J., Jimenez, M.V., Esteban, M., Baumeister, W., and Carrascosa, J.L. (2005). Cryo-electron tomography of vaccinia virus. Proc. Natl. Acad. Sci. USA *102*, 2772–2777.

Eisenmann, K.M., Harris, E.S., Kitchen, S.M., Holman, H.A., Higgs, H.N., and Alberts, A.S. (2007). Dia-interacting protein modulates formin-mediated actin assembly at the cell cortex. Curr. Biol. *17*, 579–591.

Eitzen, G. (2003). Actin remodeling to facilitate membrane fusion. Biochim. Biophys. Acta *1641*, 175–181.

Engqvist-Goldstein, A.E., and Drubin, D.G. (2003). Actin assembly and endocytosis: From yeast to mammals. Annu. Rev. Cell Dev. Biol. *19*, 287–332.

Fernandez-Borja, M., Janssen, L., Verwoerd, D., Hordijk, P., and Neefjes, J. (2005). RhoB regulates endosome transport by promoting actin assembly on endosomal membranes through Dia1. J. Cell Sci. *118*, 2661–2670.

Frischknecht, F., Moreau, V., Röttger, S., Gonfloni, S., Reckmann, I., Superti-Furga, G., and Way, M. (1999). Actin based motility of vaccinia virus mimics receptor tyrosine kinase signalling. Nature *401*, 926–929.

Frischknecht, F., and Way, M. (2001). Surfing pathogens and the lessons learned for actin polymerization. Trends Cell Biol. *11*, 30–38.

Gampel, A., Parker, P.J., and Mellor, H. (1999). Regulation of epidermal growth factor receptor traffic by the small GTPase rhoB. Curr. Biol. *9*, 955–958.

Gasman, S., Kalaidzidis, Y., and Zerial, M. (2003). RhoD regulates endosome dynamics through Diaphanous-related Formin and Src tyrosine kinase. Nat. Cell Biol. *5*, 195–204.

Geada, M.M., Galindo, I., Lorenzo, M.M., Perdiguero, B., and Blasco, R. (2001). Movements of vaccinia virus intracellular enveloped virions with GFP tagged to the F13L envelope protein. J. Gen. Virol. *82*, 2747–2760.

Harrison, S.C., Alberts, B., Ehrenfeld, E., Enquist, L., Fineberg, H., McKnight, S.L., Moss, B., O'Donnell, M., Ploegh, H., Schmid, S.L., et al. (2004). Discovery of antivirals against smallpox. Proc. Natl. Acad. Sci. USA *101*, 11178–11192.

Hiller, G., and Weber, K. (1985). Golgi-derived membranes that contain an acylated viral polypeptide are used for vaccinia virus envelopment. J. Virol. *55*, 651–659.

Hollinshead, M., Rodger, G., Van Eijl, H., Law, M., Hollinshead, R., Vaux, D.J., and Smith, G.L. (2001). Vaccinia virus utilizes microtubules for movement to the cell surface. J. Cell Biol. *154*, 389–402.

Ishizaki, T., Naito, M., Fujisawa, K., Maekawa, M., Watanabe, N., Saito, Y., and Narumiya, S. (1997). p160ROCK, a Rho-associated coiled-coil forming protein kinase, works downstream of Rho and induces focal adhesions. FEBS Lett. *404*, 118–124.

Kaksonen, M., Peng, H.B., and Rauvala, H. (2000). Association of cortactin with dynamic actin in lamellipodia and on endosomal vesicles. J. Cell Sci. *113*, 4421–4426.

Kawase, K., Nakamura, T., Takaya, A., Aoki, K., Namikawa, K., Kiyama, H., Inagaki, S., Takemoto, H., Saltiel, A.R., and Matsuda, M. (2006). GTP hydrolysis by the Rho family GTPase TC10 promotes exocytic vesicle fusion. Dev. Cell *11*, 411–421.

Lang, T., Wacker, I., Wunderlich, I., Rohrbach, A., Giese, G., Soldati, T., and Almers, W. (2000). Role of actin cortex in the subplasmalemmal transport of secretory granules in PC-12 cells. Biophys. J. *78*, 2863–2877.

Malacombe, M., Bader, M.F., and Gasman, S. (2006). Exocytosis in neuroendocrine cells: New tasks for actin. Biochim. Biophys. Acta *1763*, 1175–1183.

Manneville, J.B., Etienne-Manneville, S., Skehel, P., Carter, T., Ogden, D., and Ferenczi, M. (2003). Interaction of the actin cytoskeleton with microtubules regulates secretory organelle movement near the plasma membrane in human endothelial cells. J. Cell Sci. *116*, 3927–3938.

Moreau, V., Frischknecht, F., Reckmann, I., Vincentelli, R., Rabut, G., Stewart, D., and Way, M. (2000). A complex of N-WASP and WIP integrates signalling cascades that lead to actin polymerization. Nat. Cell Biol. *2*, 441–448.

Newsome, T.P., Scaplehorn, N., and Way, M. (2004). SRC mediates a switch from microtubule- to actin-based motility of vaccinia virus. Science *306*, 124–129.

Newsome, T.P., Weisswange, I., Frischknecht, F., and Way, M. (2006). Abl collaborates with Src family kinases to stimulate actin-based motility of vaccinia virus. Cell. Microbiol. *8*, 233–241.

Qualmann, B., and Kessels, M.M. (2002). Endocytosis and the cytoskeleton. Int. Rev. Cytol. *220*, 93–144.

Reed, N.A., Cai, D., Blasius, T.L., Jih, G.T., Meyhofer, E., Gaertig, J., and Verhey, K.J. (2006). Microtubule acetylation promotes Kinesin-1 binding and transport. Curr. Biol. *16*, 2166–2172.

Reeves, P.M., Bommarius, B., Lebeis, S., McNulty, S., Christensen, J., Swimm, A., Chahroudi, A., Chavan, R., Feinberg, M.B., Veach, D., et al.

(2005). Disabling poxvirus pathogenesis by inhibition of Abl-family tyrosine kinases. Nat. Med. *11*, 731–739.

Ridley, A.J. (2001). Rho proteins: Linking signaling with membrane trafficking. Traffic *2*, 303–310.

Rietdorf, J., Ploubidou, A., Reckmann, I., Holmström, A., Frischknecht, F., Zettl, M., Zimmermann, T., and Way, M. (2001). Kinesin dependent movement on microtubules precedes actin based motility of vaccinia virus. Nat. Cell Biol. *3*, 992–1000.

Röttger, S., Frischknecht, F., Reckmann, I., Smith, G.L., and Way, M. (1999). Interactions between vaccinia virus IEV membrane proteins and their roles in IEV assembly and actin tail formation. J. Virol. *73*, 2863–2875.

Rozelle, A.L., Machesky, L.M., Yamamoto, M., Driessens, M.H., Insall, R.H., Roth, M.G., Luby-Phelps, K., Marriott, G., Hall, A., and Yin, H.L. (2000). Phosphatidylinositol 4,5-bisphosphate induces actin-based movement of raft-enriched vesicles through WASP-Arp2/3. Curr. Biol. *10*, 311–320.

Rubinson, D.A., Dillon, C.P., Kwiatkowski, A.V., Sievers, C., Yang, L., Kopinja, J., Rooney, D.L., Ihrig, M.M., McManus, M.T., Gertler, F.B., et al. (2003). A lentivirus-based system to functionally silence genes in primary mammalian cells, stem cells and transgenic mice by RNA interference. Nat. Genet. *33*, 401–406.

Rudolf, R., Salm, T., Rustom, A., and Gerdes, H.H. (2001). Dynamics of immature secretory granules: Role of cytoskeletal elements during transport, cortical restriction, and F-actin-dependent tethering. Mol. Biol. Cell *12*, 1353–1365.

Sahai, E., and Olson, M.F. (2006). Purification of TAT-C3 exoenzyme. Methods Enzymol. *406*, 128–140.

Sampath, P., and Pollard, T.D. (1991). Effects of cytochalasin, phalloidin, and pH on the elongation of actin filaments. Biochemistry *30*, 1973–1980.

Sandilands, E., Cans, C., Fincham, V.J., Brunton, V.G., Mellor, H., Prendergast, G.C., Norman, J.C., Superti-Furga, G., and Frame, M.C. (2004). RhoB and actin polymerization coordinate Src activation with endosome-mediated delivery to the membrane. Dev. Cell *7*, 855–869.

Scaplehorn, N., Holmstrom, A., Moreau, V., Frischknecht, F., Reckmann, I., and Way, M. (2002). Grb2 and nck act cooperatively to promote actin-based motility of vaccinia virus. Curr. Biol. *12*, 740–745.

Shaner, N.C., Campbell, R.E., Steinbach, P.A., Giepmans, B.N., Palmer, A.E., and Tsien, R.Y. (2004). Improved monomeric red, orange and yellow fluorescent proteins derived from Discosoma sp. red fluorescent protein. Nat. Biotechnol. *22*, 1567–1572.

Smith, G.L., Vanderplasschen, A., and Law, M. (2002). The formation and function of extracellular enveloped vaccinia virus. J. Gen. Virol. *83*, 2915–2931.

Smith, G.L., Murphy, B.J., and Law, M. (2003). Vaccinia virus motility. Annu. Rev. Microbiol. *57*, 323–342.

Snapper, S.B., Takeshima, F., Anton, I., Liu, C.H., Thomas, S.M., Nguyen, D., Dudley, D., Fraser, H., Purich, D., Lopez-Ilasaca, M., et al. (2001). N-WASP deficiency reveals distinct pathways for cell surface projections and microbial actin-based motility. Nat. Cell Biol. *3*, 897–904.

Sodeik, B. (2000). Mechanisms of viral transport in the cytoplasm. Trends Microbiol. *8*, 465–472.

Soldati, T., and Schliwa, M. (2006). Powering membrane traffic in endocytosis and recycling. Nat. Rev. Mol. Cell Biol. *7*, 897–908.

Symons, M., and Rusk, N. (2003). Control of vesicular trafficking by Rho GTPases. Curr. Biol. *13*, R409–R418.

Taunton, J., Rowning, B.A., Coughlin, M.L., Wu, M., Moon, R.T., Mitchison, T.J., and Larabell, C.A. (2000). Actin-dependent propulsion of endosomes and lysosomes by recruitment of N-WASP. J. Cell Biol. *148*, 519–530.

Valderrama, F., Cordeiro, J.V., Schleich, S., Frischknecht, F., and Way, M. (2006). Vaccinia virus-induced cell motility requires F11L-mediated inhibition of RhoA signaling. Science *311*, 377–381.

van Eijl, H., Hollinshead, M., and Smith, G.L. (2000). The vaccinia virus A36R protein is a type Ib membrane protein present on intracellular but not extracellular enveloped virus particles. Virology *271*, 26–36.

Wallar, B.J., Deward, A.D., Resau, J.H., and Alberts, A.S. (2007). RhoB and the mammalian Diaphanous-related formin mDia2 in endosome trafficking. Exp. Cell Res. *313*, 560–571.

Ward, B.M. (2005). Visualization and characterization of the intracellular movement of vaccinia virus intracellular mature virions. J. Virol. *79*, 4755–4763.

Ward, B.M., and Moss, B. (2001a). Vaccinia virus intracellular movement is associated with microtubules and independent of actin tails. J. Virol. *75*, 11651–11663.

Ward, B.M., and Moss, B. (2001b). Visualization of intracellular movement of vaccinia virus virions containing a green fluorescent protein-B5R membrane protein chimera. J. Virol. *75*, 4802–4813.

Watanabe, N., Kato, T., Fujita, A., Ishizaki, T., and Narumiya, S. (1999). Cooperation between mDia1 and ROCK in Rho-induced actin reorganization. Nat. Cell Biol. *1*, 136–143.

Zettl, M., and Way, M. (2002). The WH1 and EVH1 domains of WASP and Ena/VASP family members bind distinct sequence motifs. Curr. Biol. *12*, 1617–1622.